Impulse Response Modeling for Underwater Wireless Optical Communication Links

Shijian Tang, *Student Member, IEEE,* Yuhan Dong, *Member, IEEE,* and Xuedan Zhang, *Member, IEEE*

***Abstract*—In underwater wireless optical communication (UWOC) links, multiple scattering may cause temporal spread of beam pulse characterized by the impulse response, which therefore results in inter-symbol interference (ISI) and degrades system error performance. The impulse response of UWOC links has been investigated both theoretically and experimentally by researchers but has not been derived in simple closed-form to the best of our knowledge. In this paper, we analyze the optical characteristics of seawater and present a closed-form expression of double Gamma functions to model the channel impulse response. The double Gamma functions model fits well with Monte Carlo simulation results in turbid seawater such as coastal and harbor water. The bit-error-rate (BER) and channel bandwidth are further evaluated based on this model for various link ranges. Numerical results suggest that the temporal pulse spread strongly degrades the BER performance for high data rate UWOC systems with on-off keying (OOK) modulation and limits the channel bandwidth in turbid underwater environments. The zero-forcing (ZF) equalization designed based on our channel model has been adopted to overcome ISI and improve the system performance. It is plausible and convenient to utilize this impulse response model for performance analysis and system design of UWOC systems.**

***Index Terms*—Underwater wireless optical communications, impulse response, Monte Carlo.**

I. Introduction

UNDERWATER wireless communications has been proposed for submarine communications due to the flexility and scalability. Underwater acoustic communications which utilizes acoustic waves to transmit information has been widely studied and implemented in the past decades. However, the channel bandwidth of underwater acoustic links is typical limited to kHz since the sound is decayed in the ocean proportionally to its frequency. And the lower propagation speed typically 1500 m/s leads to a large time delay for acoustic system. Meanwhile, the multipath reflection of sound may cause signal fading and security issues. As the frequently activities of oceanic exploitation recently, the acoustic method is not able to meet the requirements of large data and high speed communications.

Manuscript received March 14, 2013; revised September 24, 2013. The editor coordinating the review of this paper and approving it for publication was H. Haas.

This material is based on the work supported by the National Natural Science Foundation of China (No. 61201184).

This paper was presented in part at the IEEE/MTS OCEANS Conference '13, Bergen, Norway, 2013 [1].

The authors are with the Shenzhen Key Laboratory of Information Science and Technology, Department of Electronic Engineering, Tsinghua University, China. Corresponding author: Y. Dong (e-mail: dongyuhan@sz.tsinghua.edu.cn).

Digital Object Identifier 10.1109/TCOMM.2013.120713.130199

In recent years, underwater wireless optical communications (UWOC) has attracted considerable attentions as an alternative technology to traditional acoustic approach. As a special type of free space optical (FSO) communications, UWOC systems employ the blue/green region of visible light spectrum to realize data transmission since this region of light suffers lowest attenuation in natural water [2]. Compared with acoustic communications, UWOC systems can provide high security, low time delay and a much higher data rate up to hundreds of Mbps [3] in relatively short ranges (typically shorter than 100 meters). Due to these advantages, UWOC has numerous applications such as real-time video communications, remote sensing and navigation, imaging as well as high throughput sensor network.

Prior studies have shown that the optical beam suffers absorption and scattering through propagation in the seawater [2]. The absorption and scattering may introduce the effects of energy loss and direction changing for the optical beams, respectively. In turbid medium especially coastal and harbor water, the transmitted photons are scattered multiple times, which is referred to as multiple scattering [4]. The multiple scattering effect may spread beam pulse both temporally and spatially, which plays a key role in beam propagation. The spatial beam spreading has been studied in [5] and exerts a positive impact on system performance [6], [7]. However, the temporal beam spreading will introduce the temporal dispersion and therefore corrupt the receive signal especially for turbid water types [4], [8].

In this paper, we focus on the temporal dispersion of UWOC links and investigate the effect of corresponding impulse response. More recently, the impulse response of underwater optical links has been studied theoretically and experimentally. Most prior works [3], [9]–[12] have adopted Monte Carlo approach to model the impulse response of UWOC links. And [13] has validated Monte Carlo approach on modeling the UWOC impulse response by experimental measurement. Instead of Monte Carlo method, Jaruwatanadilok [14] developed an analytical model of impulse response based on the vector radiative transfer theory.

However, to the best of our knowledge, these prior works have not provided simple closed-form expressions of impulse response of UWOC links, i.e., the impulse response could only be obtained numerically. Wei *et al.* [15] have proposed an inverse Gaussian function to model the impulse response of UWOC links. However, their results are limited in small link ranges and clean water and not based on the actual measurement data of seawater parameters. Furthermore, their work only focused on the half amplitude width extension

between the transmit and receive pulses in time domain without comparing the theoretical shape of impulse response with that from either Monte Carlo simulations or experiment. In this paper, we focus on the impulse response of relatively turbid water types such as coastal and harbor water where the temporal dispersion can not be ignored and will affect the system performance. The double Gamma functions has been firstly adopted in modeling the impulse response of FSO links through fog [16], [17] and then applied to model the impulse response in dispersive medium characterized by Henyey-Greenstein (HG) function [2] in our earlier work [1]. Although seawater has different properties from the medium studied in these prior works, they are dispersive medium through which the light may suffer the effect of multiple scattering. Therefore we analyze the optical properties of seawater, firstly apply the double Gamma functions to model the impulse response of UWOC links which fits well with the Monte Carlo simulation results in coastal and harbor water and further investigate the valid region of this model. Then based on the double Gamma functions model, we analyze and evaluate the system performance of inter-symbol interference (ISI), channel bandwidth as well as the bit-error-rate (BER). Numerical results suggest that the temporal pulse spread strongly degrades the BER performance without equalization based on on-off keying (OOK) modulation for long link range and high data rate such as 1 Gbps of the 40 m link in coastal water or 800 Mbps of the 10 m link in harbor water.

To eliminate the detrimental effect of ISI and improve the BER performance, equalization has been employed in atmospheric FSO links [18], [19] and indoor infrared links [20]. In this study, we apply the simplest and most widely used zero-forcing (ZF) equalization based on double Gamma functions model to enhance the error performance of the high speed UWOC system operating in seawater environment in the presence of ISI.

Based on our study, the temporal dispersion for underwater optical links can be estimated and analyzed by the double Gamma functions model. Compared with Monte Carlo approach, the double Gamma functions model can strongly facilitate the evaluation of BER performance, equalization and 3-dB channel bandwidth due to the simplicity of its closed-form expression, which is plausibly beneficial to the design of UWOC systems and link performance analysis.

The rest of paper is organized as follows. In Section II, we introduce the characteristics of seawater and system model of UWOC links as well as each component of noise. Then, in Section III, we summarize the basic rules of Monte Carlo approach and present a simple closed-form model for the impulse response of UWOC links using double Gamma functions. Finally, we evaluate the link performance for UWOC systems based on this impulse response model in Section IV and draw the the conclusions in Section V.

II. Link Characteristics and System Model

A. Optical Characterization of Seawater

The interactions between each photon and seawater contain absorption and scattering through beam propagation. Absorption is an irreversible process where the energy of photons lost thermally by interacting with water molecule and other particles. In scattering process, the transmit direction of each photon is changed by the interactions between photons and seawater, which may cause energy loss since less photons are captured by the receiver. The energy loss of the non-scattered light caused by absorption and scattering processes can be evaluated by absorption coefficient $a(\lambda)$ and scattering coefficient $b(\lambda)$, respectively. The extinction coefficient (also known as attenuation coefficient in ocean optics) $c(\lambda) = a(\lambda) + b(\lambda)$ describes the total effects of absorption and scattering on energy loss. The values of $a(\lambda)$, $b(\lambda)$ and $c(\lambda)$ vary with the water type and source wavelength λ.

Unlike the FSO links in atmosphere, the UWOC links encounter a large number of suspended particles such as dissolved salts, mineral components, organic matter and etc. in underwater environment. Then the scattering order of light is typically high in seawater especially in coastal and harbor water. There exist three types of scattering in water [2] such as small scale scattering ($\ll \lambda$) caused by density fluctuations due to random molecular motions (also known as pure seawater scattering), particle scattering by large suspended particles ($> \lambda$), and large scale scattering ($\gg \lambda$) resulting from turbulence-induced refractive fluctuations. Note that the large scale scattering caused by turbulence has not been fully studied yet and is omitted by most prior works in UWOC. In this paper, we therefore only consider the pure seawater scattering and particle scattering with coefficients $b_{sw}(\lambda)$ and $b_p(\lambda)$, respectively, which implies the total scattering coefficient $b(\lambda) = b_{sw}(\lambda) + b_p(\lambda)$.

To study the effects of multiple scattering, the scattering phase function (SPF) $\beta(\theta, \lambda)$ is introduced to describe the energy distribution of scattering light versus scattering angle θ with

$$1 = 2\pi \int_0^{\pi} \beta(\theta, \lambda) \sin\theta d\theta \tag{1}$$

Since we mainly focus on the propagation of blue/green region of visible light, we simply omit the parameter λ for brevity hereafter.

The SPF of small scale scattering has the form similar to typical Rayleigh scattering with corrections of anisotropy of water molecules as [2],

$$\beta_{sw}(\theta) = 0.06225(1 + 0.835\cos^2\theta) \tag{2}$$

Taking into account the particle scattering caused by large suspended organic or inorganic particles, seawater SPF is strongly peaked in small forward angles and measured by Petzold [21] for selected water types. Several closed-form expressions have been adopted to represent the SPF of seawater such as HG function and two terms HG (TTHG) function [10].

The HG function [2] is typically used to describe the SPF of dispersive medium such as clouds with the expression as

$$\beta_{\mathrm{HG}}(\theta) = \frac{1 - g^2}{4\pi(1 + g^2 - 2g\cos\theta)^{\frac{3}{2}}} \tag{3}$$

where θ is the scattered angle and g is the average cosine of θ. However, the HG function differs from Petzold's measurement of seawater SPF especially in small forward angles ($<20^\circ$) and backward angles ($>130^\circ$) [10], and therefore underestimates the forward and backward scattering light. TTHG function is

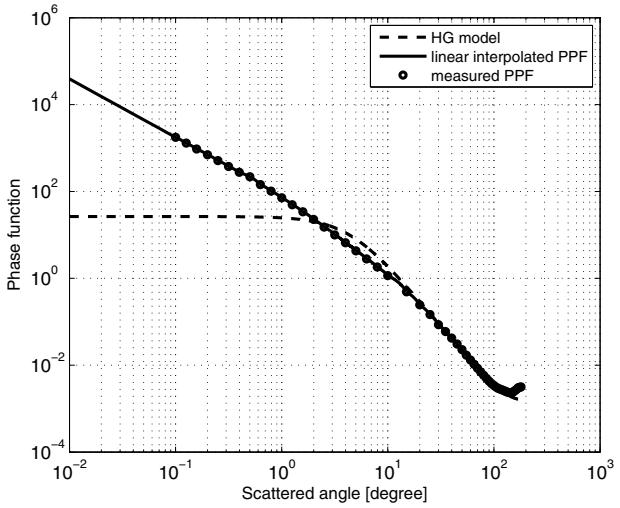

Fig. 1. Particle phase function from [2] and SPF of the HG model.

a modification of HG function and has slight improvement in small forward angles [10]. However, the outputs of TTHG function are much smaller than the Petzold's measurement for angles below 1° and larger than the measurement for angles above 140° as [10, Fig. 3] indicated. Thus, we adopt the measured value of Petzold in [21] as the seawater SPF of particles in this paper rather than both HG and TTHG functions.

Mobley [2] averaged the measurement based on Petzold's results for different water types and subtracted the effects of pure seawater to obtain the SFP for particle scattering which is also referred to as particle phase function (PPF). To release the restriction of limited data points of measured PPF, Mobley then proposed a scheme by utilizing linear interpolation for $\theta \geq 0.1^\circ$ and the assumption that the PPF is proportional to $\theta^{-1.346}$ for $\theta < 0.1^\circ$, and also confirmed the validity of (1) [2]. By this means, the PPF can be added more data points, which is referred to as linear interpolated PPF hereafter for simplicity. The results obtained based on the rules above are adopted in this paper to represent the PPF denoted as $\beta_p(\theta)$.

Fig. 1 shows the measured PPF and linearly interpolated PPF as well as the SPF of HG model (3) with $g = 0.924$ for comparison. In this figure, PPFs are close to SPF of HG model for large scattered angles, otherwise an obvious gap exists. Note that the pure seawater scattering has little contribution to the SPF with details will be provided in the following discussion. Therefore, the SPF of our model deviates slightly from the linear interpolated PPF in Fig. 1.

The total SPF $\beta(\theta)$ including the effects of pure seawater and particles is given by,

$$\beta(\theta) = \frac{b_{sw}}{b}\beta_{sw}(\theta) + \frac{b_p}{b}\beta_p(\theta) \tag{4}$$

In this paper, we mainly focus on the temporal pulse spread in turbid environments such as coastal and harbor water with channel parameters summarized in Table I [2]. The typical value of b_{sw} is 2.33×10^{-3} m^{-1} for blue/green region of visible light spectrum [2], which implies the particle scattering coefficient $b_p \gg b_{sw}$ and little contribution to the SPF made by small scale scattering.

TABLE I
PARAMETERS FOR BLUE/GREEN LIGHT IN COASTAL AND HARBOR WATER

Water type	a [m^{-1}]	b [m^{-1}]	c [m^{-1}]
Coastal	0.179	0.219	0.398
Harbor	0.366	1.824	2.190

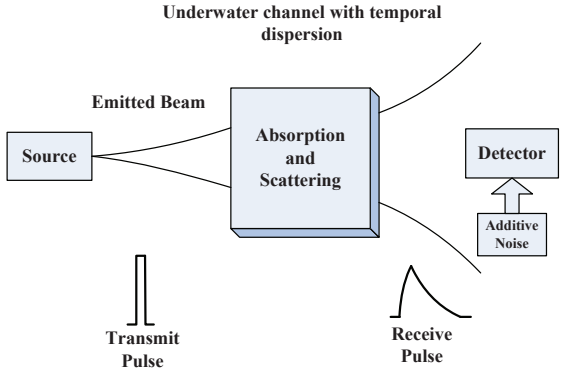

Fig. 2. System model and link geometry of the UWOC link.

Generally, the processes of absorption and multiple scattering of light propagation in seawater can be described theoretically by the radiative transfer equation (RTE) [22], which can be solved both numerically and analytically.

B. System Model

In this section, we present the system model for UWOC links as well as the general link geometry. As shown in Fig. 2, we consider a UWOC system with a precisely aligned line-of-sight (LOS) link and receiver locating on the plane perpendicular to the beam axis. The beam pulse emitted from the source is deteriorated temporally through the underwater channel, and then corrupted by the noise in the receiver reception.

In our analysis, the underwater environment is assumed to be an ideal isotropic and homogeneous medium without flowing and turbulence. Therefore underwater wireless optical channel can be treated as a linear time-invariant system [14]. Note that the actual underwater optical channel is more complex when we consider the temporal correlation of irradiance caused by medium flowing as well as fading effects induced from both turbulence and random distribution of particles [23].

The noise of UWOC systems depends on the type of receiver. For an ideal photon counting receiver [24] where the number of detected photons in each slot follows the Poisson distribution, the receiver noise has sources mainly from the background radiation and dark current. For a more realistic receiver with the photon detector and load electronic devices, the receiver noise is a combination of background radiation noise, shot noise, dark current noise, and thermal noise, which can be approximated and modeled as additive white Gaussian noise (AWGN) [14], [18], [19]. In this paper, with the assumption of AWGN at the receiver, the UWOC system can be modeled as [14]

$$y(t) = h(t) * x(t) + n(t), \tag{5}$$

where $x(t)$ and $y(t)$ are the transmit and receive signal, respectively, $h(t)$ is the impulse response of UWOC links, $n(t)$ is the AWGN, and $*$ denotes the convolution operator.

The receive current noise in our work takes into account the effects of background radiation, dark current, shot noise and thermal noise, which can be estimated based on prior studies [14], [25], [26] with the noise variances given by

$$\begin{aligned} \sigma_0^2 &= \sigma_b^2 + \sigma_d^2 + \sigma_t^2 \\ \sigma_1^2 &= \sigma_b^2 + \sigma_d^2 + \sigma_s^2 + \sigma_t^2 \end{aligned} \tag{6}$$

where σ_0^2 and σ_1^2 represent the variance of the noise for empty and pulse slots, respectively. σ_b^2, σ_d^2, σ_t^2 and σ_s^2 are the variances of background radiation, dark current, thermal noise and shot noise, respectively. The exact noise distribution can be found in [27] for the realistic devices such as avalanche photodiode (APD), which is out of the scope of this paper.

III. Impulse Response Modeling

A. Monte Carlo Simulation

As a numerical solution of RTE, Monte Carlo approach employs the statistical method to evaluate the channel characteristics by generating numerous photons and then simulating the interactions of each photon with the medium. Compared with the analytical solutions of RTE, Monte Carlo approach is more flexible for various link geometry without restrictions on the scattering angles and therefore is widely employed in simulating the light propagation in dispersive medium, e.g., beam propagation in seawater [11], [13].

We adopt the Monte Carlo approach similar to [11], [28] with basic rules summarized as follows. Initially, a set of photons is emitted by the source with specific divergence angle. The interactions for each photon with the medium contain absorption and scattering and can be modeled by changing the basic attributes of each photon such as the position, transmit direction, propagation time and weight during the propagation. These attributes are recorded when the photon reaches the receiver. By collecting and analyzing the basic attributes for all received photons statistically, we can obtain the channel characteristics such as impulse response and path loss. Detailed steps are provided in the following section.

The basic attributes of each photon include the photon position in Cartesian coordinates (x, y, z), the direction of transmission described by zenith angle θ and azimuth angle ϕ[1], propagation time t and weight w. For the source with narrow emission aperture, each photon is initialized at the position $(0, 0, 0)$ with zero start time and unit weight. The emitted direction of each photon depends on both the divergence angle and angular intensity distribution of the source with details in [11].

Each photon may interact with the medium when propagating Δs distance, which can be determined by $\Delta s = -\ln \xi_s / c$ with ξ_s as an uniform distributed random variable in the interval of $[0, 1]$. After the distance between two interactions Δs being determined, the spatial position and propagation time can be updated accordingly [11]. The photon weight can be updated by

$$W^{i+1} = \left(1 - \frac{a}{c}\right) W^i \tag{7}$$

where W^i is the photon weight after the i th interaction with medium. The scattering may also affect the direction of photon trajectory which changes with the scattering zenith angle θ_s as

$$\xi_\theta = 2\pi \int_0^{\theta_s} \beta(\theta) \sin\theta d\theta \tag{8}$$

where ξ_θ is an uniform distributed random between 0 and 1 with $\beta(\theta)$ as the SPF. θ_s can be obtained by solving (8) numerically.

Then the scattering azimuth angle ϕ_s can be computed by

$$\phi_s = 2\pi\xi_\phi \tag{9}$$

where ξ_ϕ is also an uniformly distributed random variable in $[0, 1]$. Note that the scattering angles in (8) and (9) are the relative rotation angles to the direction before interactions. Hence, the next step is to transfer the direction of the photon into the absolute coordinate system [11].

The tracking of each photon should be stopped either the photon reaches the receiver plane[2] or its weight is lower than certain threshold. In the former case, the attributes including position, direction, propagation time and weight are recorded for each photon. In the latter case, the photon should be excluded from the simulation as [10], [11] suggested since the photons with lower weight than threshold have negligible contribution to the total receive photons. We set the value of photon weight threshold as 10^{-6} and have verified that this value is sufficient for the results of all scenarios in this paper.

As [11] indicated, the photon reception can be treated as photon selection. When the photons reach the receiver plane, only the ones within the receiver aperture and with zenith angles less than the half angle of receiver FOV are selected as the detected photons.

After repeating the steps above for each photon and recording all the attributes for detected photons, the histogram of received intensity versus propagation time for unit transmit intensity can be estimated by summing the weight of photons with the same propagation time and then normalized by the total transmit weight, which is equivalent to the channel impulse response. By this reason, the time resolution corresponds to the temporal bin size of this histogram and is set to $t_d = 10^{-10}$ s which implies the same achievable receiver sample rate of 20 GSps as the digital receiver in [13].

B. Double Gamma Functions Model

In this section, we will present the closed-form expression of the impulse response for UWOC links. Based on the measurement in [29], the energy transportation in UWOC links can be divided into two regions where the non-scattering and multiple scattering light are dominant, respectively. For small values of the attenuation length (also known as optical thickness) τ defined as $\tau = cL$ [5] with c as the extinction coefficient and L as the physical link range, the non-scattering

[1] θ is defined as the angle between the direction of photon and z axis, and ϕ is the angle between the project of direction on xOy plane and x axis

[2] The receiver locates in the receiver plane perpendicular to the beam axis in our link geometry.

light dominates at the receiver side where the path loss versus τ follows the Beer's law [2]. As τ increases, the transition between these two regions occurs, after which the multiple scattering light dominates and the path loss deviates from Beer's law. [29] also implies negligible temporal dispersion of UWOC links in the non-scattering light dominating region, which is verified in [9], [10] by simulating the impulse response in clean water, and increasing temporal dispersion in the multiple scattering light dominating region as τ increases. In this work, we mainly focus on the impulse response modeling of UWOC links in coastal and harbor water environment where τ has relatively large values.

The double Gamma functions has been firstly adopted to model the impulse response in clouds [16] where τ is no less than 20. Although the channel properties of seawater differ from clouds [2], motivated by the dispersive nature of these two medium, we apply the double Gamma functions to model the impulse response in UWOC links with relatively large value of τ where multiple scattering light may dominate. The closed-form expression of the double Gamma functions is

$$h(t) = C_1 \Delta t e^{-C_2 \Delta t} + C_3 \Delta t e^{-C_4 \Delta t}, \quad (t \geq t_0) \tag{10}$$

where C_1, C_2, C_3 and C_4 are the four parameters to be solved. And $\Delta t = t - t_0$ where t is the time scale and $t_0 = L/v$ is the propagation time which is the ratio of link range L over light speed v in water.

The parameter set (C_1, C_2, C_3, C_4) in (10) can be computed from Monte Carlo simulation results using nonlinear least square criterion as

$$(C_1, C_2, C_3, C_4) = \arg\min \left(\int \left[h(t) - h_{mc}(t) \right]^2 dt \right) \tag{11}$$

where $h(t)$ is the double Gamma functions model in (10) and $h_{mc}(t)$ is the Monte Carlo simulation results of impulse response. $\arg\min(\cdot)$ is the operator to return the argument of the minimum. Then (11) can be solved by curve fitting approach using scientific computing software such as MATLAB and etc.

Some prior works have used a single Gamma function to model the impulse response for the non-line-of-sight (NLOS) link geometry [30] or the links with $\tau > 31$ [31]. The light field may be too diffused in these scenarios, which can be treated as a special case of double Gamma functions model.

We consider a 532 nm source with 10° divergence angle (full angle) and a photon detector with 50 cm aperture [9]. Instead of the collimated source or compact aperture, we choose the divergent source and wide aperture aim to increase the temporal dispersion. The relationship between system configurations (such as source divergence, aperture size and FOV) and the validation of our model will be discussed in details later. The system geometry is a precisely aligned LOS link with receiver locating at the plane perpendicular to the beam axis. Based on these settings, we simulate the beam propagation of various link ranges and FOV in coastal and harbor water by the Monte Carlo method using at least 10^9 photons for each scenario. Then the impulse response is obtained and fitted by the expression in (10). We choose the results of four link ranges shown in Figs. 3 and 4. Note that in Figs. 3 and 4, the start time of impulse response is shifted from t_0 to zero, and the time interval of observation is set to $[0, 6]$ ns in all subfigures for a convenient comparison. Then the temporal dispersion which is defined similarly to [9] as the time interval of impulse response falling 20 dB below the peak can be evaluated from double Gamma functions model for various link ranges, water types and FOVs as shown in Table II.

TABLE II
TEMPORAL DISPERSION IN UNITS OF NS FOR VARIOUS LINK RANGES, WATER TYPES AND FOVS.

Coastal			Harbor		
FOV	$L = 30$ m	$L = 40$ m	FOV	$L = 10$ m	$L = 12$ m
20°	1.23 ns	2.04 ns	20°	2.77 ns	4.95 ns
40°	1.65 ns	3.01 ns	40°	4.00 ns	7.27 ns
180°	1.90 ns	3.51 ns	180°	6.98 ns	11.85 ns

Figs. 3 and 4 demonstrate that the double Gamma functions fits well with the simulated impulse response regardless of link range, FOV and water type. Fig. 3 depicts the temporal pulse spread due to the effect of multiple scattering. Comparing the results of impulse response for different link ranges in coastal water shown in Fig. 3 and Table II, we can find that the impulse response disperses more heavily as the attenuation length increases. This is intuitive since the photons suffer more scattering for longer propagation distance and the intensity of impulse response also reduces as the photons undergo more attenuation. Similar results in harbor water can be observed in Fig. 4 and Table II. Additionally, the temporal dispersion of impulse response decreases as FOV decreases as shown in Table II. We have verified that the receiver with narrow FOV cannot detect the photons which are typically scattered multiple times during the long time propagation and therefore result in large arrival angles (defined as the angle between the propagating direction of a photon and beam axis).

The root mean square errors (RMSE) of impulse response by double Gamma functions for each scenario with 180° FOV are summarized in Table III. We have also verified that the RMSE for each scenario with other FOVs such as 20° and 40° are still less than 5%. Hence we can conclude that the double Gamma functions can well model the impulse response of UWOC LOS links, which benefits the system design and performance evaluation of UWOC systems.

As mentioned earlier, [29] has implied the dependence of the transition between non-scattering and multiple scattering light dominant regions on water types and system configurations such as source divergence, receiver aperture and FOV. For simplicity, the UWOC systems with relatively large divergence of source, large receiver aperture size and wide FOV are referred to as wide configuration systems while the UWOC systems with relatively small divergence of source, compact receiver and narrow FOV are referred to as narrow configuration systems. For wide configuration systems and specific water types, it is intuitive that the multiple scattering light with large displacement or arrival angle still can reach the receiver and therefore may dominate even at relatively small τ. On the other hand, for narrow configuration systems with not large enough τ, the impulse response can be approximately modeled by an ideal delta function (denoted as $A\delta(t)$ with the path loss A and typically used to model the system impulse

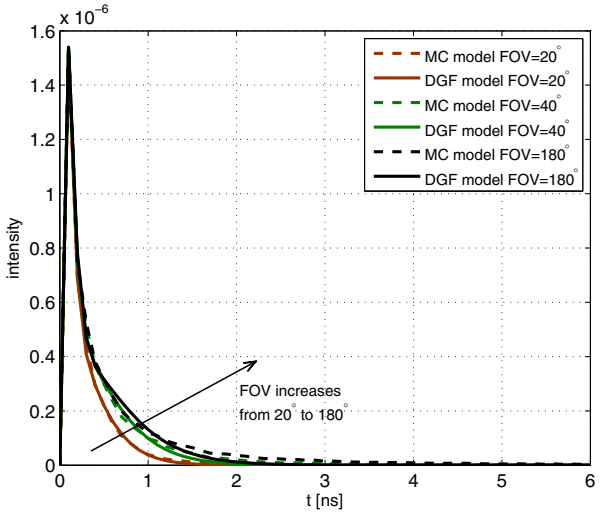

(a) 30 m link range.

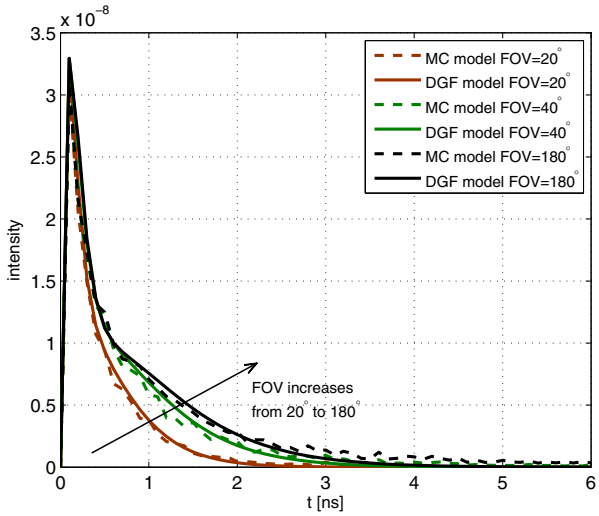

(b) 40 m link range.

Fig. 3. Impulse response in coastal water (MC and DGF denote Monte Carlo and double Gamma Functions respectively).

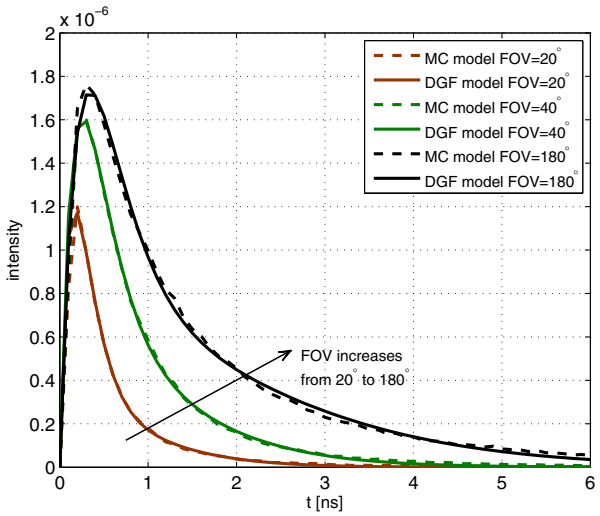

(a) 10 m link range.

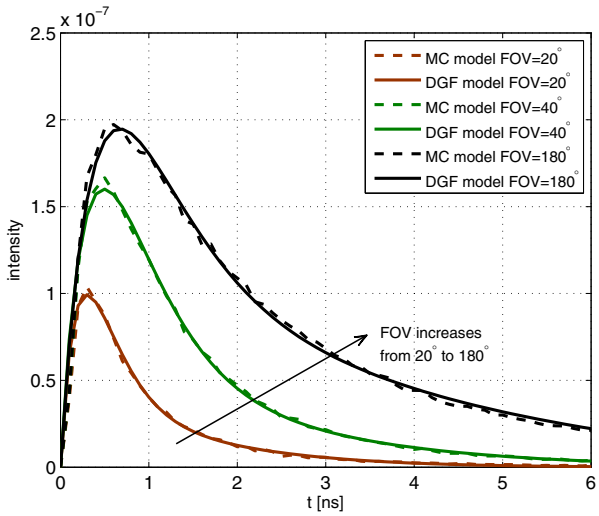

(b) 12 m link range.

Fig. 4. Impulse response in harbor water (MC and DGF denote Monte Carlo and double Gamma Functions respectively).

response without ISI) due to the negligible temporal dispersion. In this case, the double Gamma functions model may therefore break down. Extra simulations for various link ranges and system configurations have been done in both coastal and harbor water, respectively. By simulating the impulse response for narrow configuration systems, we have verified that the double Gamma functions will be valid only for relatively large τ corresponding to turbid water type or large link range where the temporal dispersion is innegligible and therefore the ideal delta function without ISI is no longer suitable to describe the system. For wide configuration systems, however, the double Gamma functions model will not break down even for relatively small τ and be valid obviously for large τ. Unfortunately, the exact relationship among transition, water types and system configurations still remains unknown to the best of our knowledge. Therefore the exact valid region of double Gamma functions model for various water types and system configurations deserves our future studies and is beyond the scope of this paper.

TABLE III
CURVE FITTING RESULTS FOR VARIOUS LINK RANGES IN COASTAL AND HARBOR WITH 180° FOV.

Coastal		Harbor	
Link range L	RMSE	Link range L	RMSE
30 m	0.01405	10 m	0.01552
40 m	0.01141	12 m	0.01692
50 m	0.04276	14 m	0.01783
60 m	0.02481	16 m	0.02791

TABLE IV
COEFFICIENTS FOR OUR SYSTEM

Coefficient	Value
Quantum efficiency η	0.8
Wavelength of the source λ	532 nm
Electronic bandwidth B	20 GHz
Dark current $I_{\rm dc}$	1.226 nA
Noise figure F	4
Equivalent temperature T_e	290 K
Load resistance R_L	100 Ω

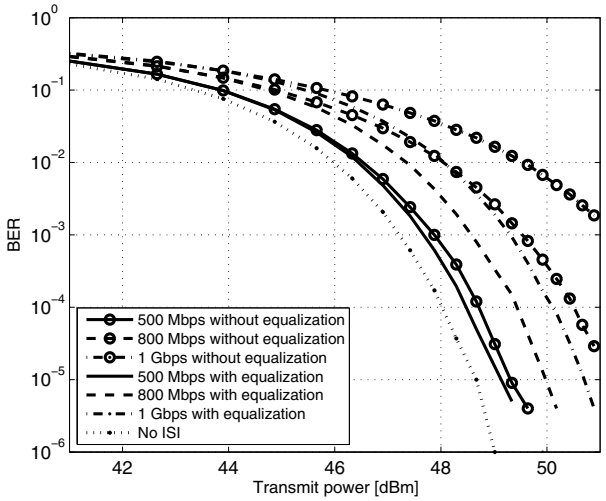

Fig. 5. BER performance versus transmit power of 40 m link in coastal water with 180° FOV.

IV. PERFORMANCE EVALUATION

In this section, we present the performance analysis of UWOC systems directly based on the simple closed-form model of the impulse response developed in the previous section. We first evaluate the ISI effect as well as BER performance, and then calculate the channel bandwidth for coastal and harbor water. The parameters for system configuration are listed in Table IV.

A. BER Performance

We consider an UWOC system operating in turbid water environment in the presence of ISI. The transmitter intends to transmit data using OOK scheme, i.e., representing the low bits and high bits by empty and pulse slots respectively. The ISI introduced by the temporal spread of beam pulse degrades the system performance and can be analyzed equivalently at baseband regardless of the presence of ISI with details in [20]. Similar to [14], the detection process can be modeled by integrating the received signal over the slot duration and adding the noise estimated in (6). Then the output sequence of the detection process is sent through the ZF equalizer where its tap weights depend on the channel impulse response according to the basic rules given by [32, Eqs. (9.4-5)-(9.4-7)].

We evaluate the BER performance based on ZF equalization by Monte Carlo approach which generates and sends at least 10^6 equiprobable bits through the underwater channel modeled

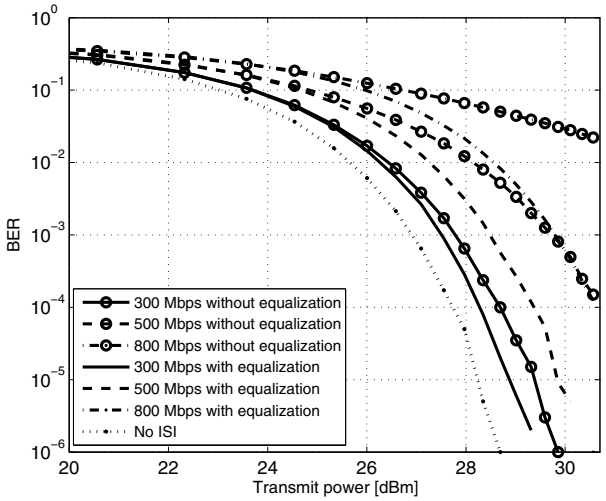

Fig. 6. BER performance versus transmit power of 10 m in harbor water with 180° FOV.

by double Gamma functions as in (10) for each type of coastal and harbor water. For comparison, we also simulate the BER performance in the absence of equalization as [20] suggested. Figs. 5 and 6 show the BER performance versus transmit power with various link ranges, water types and bit rates. Aim to study the worst case of signal degradation caused by the temporal dispersion, we only consider the receiver with 180° FOV. The transmit power is defined as the average transmit power of the pulse slots after OOK modulation. From these two figures, we can observe the detrimental effect of ISI especially for high data rates and large attenuation lengths without equalization. For instance, when the bit rate is as high as 1 Gbps for 40 m link in coastal water or 800 Mbps for 10 m link in harbor water, the BER performance strongly degrades without equalization. Figs. 5 and 6 suggest that the ZF equalization scheme can eliminate the detrimental effect of ISI and improves the BER performance regardless of link ranges, water types as well as bit rates. Note that the BER performance may be further enhanced when the decision feedback equalization (DFE) or mean square error (MSE) criterion are adopted [32] which is beyond the scope of this paper. The relationship among BER performance, equalization schemes, data rates, channel parameters and system configurations deserves a thorough study and will be our future work.

B. Channel Bandwidth

The closed-form expression of the impulse response provides an easy way to determine the channel bandwidth which implies frequency bandwidth available for communications. The channel bandwidth for coastal and harbor can be directly calculated based on the double Gamma functions model of channel impulse response. Taking a Fourier transform of (10) yields the frequency response as

$$H(2\pi f) = \frac{C_1}{(j2\pi f + C_2)^2} e^{-j2\pi f t_0} + \frac{C_3}{(j2\pi f + C_4)^2} e^{-j2\pi f t_0} \tag{12}$$

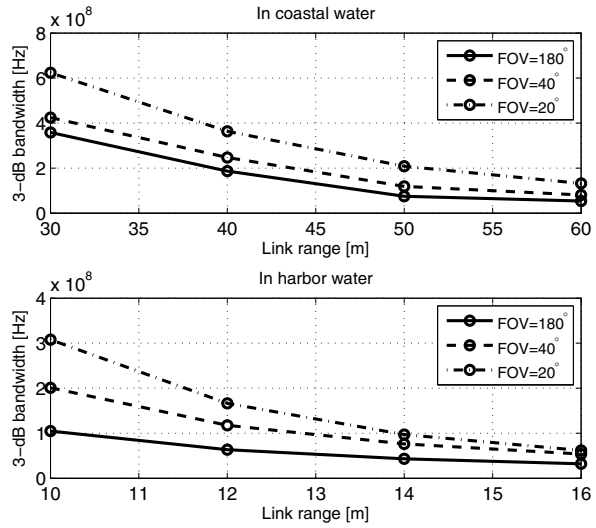

Fig. 7. 3 dB channel bandwidth versus link range.

where f is the frequency in unit of Hz and j is the imaginary unit. The 3 dB channel bandwidth can be computed by solving the following equation.

$$|H(2\pi f_{3\mathrm{dB}})|^2 = \frac{1}{2}|H(0)|^2 \tag{13}$$

where $f_{3\mathrm{dB}}$ is the 3 dB bandwidth to be determined, and $|H(0)|$ is value of amplitude frequency response corresponding to $f = 0$.

By solving (13) numerically, the channel bandwidth for various link ranges in coastal and harbor water is illustrated in Fig. 7. From this figure, we can observe that the channel bandwidth decreases for large link range or turbid water type as the temporal dispersion increases for large attenuation length. The receiver with narrow FOV will omit the photons with long propagation time and large arrival angles, and therefore enhance the performance of channel bandwidth regardless of water types and link ranges by decreasing the temporal dispersion.

Based on the channel bandwidth performance, it is intuitive that although the optical link can provide higher data rate than acoustic one, the channel dispersive characteristic will still limit the data rate for turbid environment such as coastal and harbor water. Therefore, equalization technique designed on our model is necessary to be utilized to improve the system performance for the scenarios with high bit rate and large attenuation length.

V. Conclusion

In this paper, we have investigated the temporal dispersion of UWOC links due to the multiple scattering effect in turbid environments. A closed-form expression of double Gamma functions is presented to model the channel impulse response, which fits well with the Monte Carlo simulations using actual SPF for various link ranges in coastal and harbor water. This provides a plausible and convenient way to evaluate the system performance such as BER and bandwidth based on this simple closed-form model of impulse response. Numerical results suggest that the 3-dB channel bandwidth decreases for large attenuation lengths where light suffers much temporal spreading, meanwhile the ISI degrades BER performance heavily for high bit rates system without equalization. ZF equalizer designed based on the double Gamma functions model has been adopted in high speed UWOC systems and validated to improve the BER performance of system. The experimental verification, UWOC ISI channel capacity, exact relationship between the parameters in double Gamma functions model and link configurations such as water types, source divergence, receiver aperture and FOV, etc. will be our future work.

References

[1] S. Tang, X. Zhang, and Y. Dong, "On impulse response for underwater wireless optical communication links," in *Proc. 2013 IEEE/MTS OCEANS Conf.*, pp. 1–4.

[2] C. Mobley, *Light and Water: Radiative Transfer in Natural Waters*. Academic Press/Elsevier Science, 1994.

[3] F. Hanson and S. Radic, "High bandwidth underwater optical communication," *Appl. Opt.*, vol. 47, no. 2, pp. 277–283, 2008.

[4] B. M. Cochenour and L. J. Mullen, "Free-space optical communications underwater," in *Advanced Optical Wireless Communication System,* pp. 201–239. Cambridge University Press, 2012.

[5] B. M. Cochenour, L. J. Mullen, and A. E. Laux, "Characterization of the beam-spread function for underwater optical communications links," *IEEE J. Ocean. Eng.*, vol. 33, no. 4, pp. 513–521, Oct. 2008.

[6] S. Tang, Y. Dong, and X. Zhang, "On link misalignment for underwater wireless optical communications," *IEEE Commun. Lett.*, vol. 16, no. 10, pp. 1688–1690, Oct. 2012.

[7] S. Arnon "Underwater optical wireless communication network," *Opt. Eng.,* vol. 49, no. 1, pp. 015001-1-6, 2010.

[8] B. Cochenour and L. Mullen, "Channel response measurements for diffuse non-line-of-sight (NLOS) optical communication links underwater," in *Proc. 2011 IEEE OCEANS Conf.*, pp. 1–5.

[9] C. Gabriel, M. Khalighi, S. Bourennane, P. Leon, and V. Rigaud, "Channel modeling for underwater optical communication," in *Proc. 2011 IEEE Workshop on Optical Wireless Communications, Globecom Conf.*, pp. 833–837.

[10] C. Gabriel, M. Khalighi, S. Bourennane, P. Leon, and V. Rigaud, "Monte-Carlo-based channel characterization for underwater optical communication systems," *J. Opt. Commun. Netw.,* vol. 8, no. 1, pp. 1–12, 2013.

[11] W. Cox, "Simulation, modeling, and design of underwater optical communication systems," Ph.D. dissertation, North Carolina State University, Raleigh, 2012.

[12] J. Li, Y. Ma, Q. Zhou, B. Zhou, and H. Wang, "Monte Carlo study on pulse response of underwater optical channel," *Optical Engineering*, vol. 51, no. 6, 066001-5, 2012.

[13] F. Dalgleish, F. Caimi, and A. Vuorenkoski, "Efficient laser pulse dispersion codes for turbid undersea imaging and communications applications," in *Proc. SPIE*, vol. 7678, 2010, pp. 1–12.

[14] S. Jaruwatanadilok, "Underwater wireless optical communication channel modeling and performance evaluation using vector radiative transfer theory," *IEEE J. Sel. Areas Commun.*, vol. 26, no. 9, pp. 1620–1627, Dec. 2008.

[15] W. Wei, X. Zhang, J. Rao, and W. Wang, "Time domain dispersion of underwater optical wireless communication," *Chin. Opt. Lett.,* vol. 9, pp. 030101, 2011.

[16] G. Mooradian and M. Geller, "Temporal and angular spreading of blue-green pulses in clouds," *Applied Optics*, vol. 21, no. 9, pp. 1572–1577, May 1982.

[17] M. Aharonovich and S. Arnon, "Performance improvement of optical wireless communication through fog with a decision feedback equalizer," *J. Opt. Soc. Am. A,* vol. 22, pp. 1646–1654, 2005.

[18] C. Reinhardt, Y. Kuga, S. Jaruwatanadilok, and A. Ishimaru, "Improving bit-error-rate performance of the free-space optical communications system with channel estimation based on radiative transfer theory," *IEEE J. Sel. Areas Commun.*, vol. 27, no. 9, pp. 1591–1598, Dec. 2009.

[19] C. Reinhardt, S. Jaruwatanadilok, Y. Kuga, A. Ishimaru, and J. Ritcey, "Investigation of multilevel amplitude modulation for a dual-waveleng th free-space optical communications system using realistic channel estimation and minimum mean-squared-error linear equalization," *Applied Optics*, vol. 47, no. 29, pp. 5378–5389, Oct. 2008.

[20] J. M. Kahn, W. J. Krause, and J. B. Carruthers, "Experimental characterization of non-directed indoor infrared channels," *IEEE Trans. Commun.*, vol. 43, no. 2/3/4, pp. 1613–1623, 1995.
[21] T. Petzold, "Volume scattering functions for selected ocean waters," SIO Ref. 72-78, Scripps Institution of Oceanography Visibility Laboratory, San Diego, CA, Oct. 1972.
[22] W. H. Wells, "Loss of resolution in water as a result of multiple small angle scattering," *J. Opt. Soc. Amer.*, vol. 59, no. 6, pp. 686–691, 1969.
[23] L. Andrews and R. Phillips, *Laser Beam Propagation through Random Media*, 2nd ed. SPIE Press, 2005.
[24] S. Wilson, M. Pearce, and Q. Cao, "Optical repetition MIMO transmission with multipulse PPM," *IEEE J. Sel. Areas Commun.*, vol. 23, no. 9, pp. 1901–1910, Sep. 2005.
[25] J. Giles and I. Bankman, "Underwater optical communications systems—part 2: basic design considerations," in *Proc. 2005 IEEE MILCOM Conf.*, pp. 1700–1705.
[26] H. Manor and S. Arnon, "Performance of an optical wireless communication system as a function of wavelength," *Applied Optics*, vol. 42, no. 21, pp. 4285–4294, July 2003.
[27] P. Webb, R. Mclntyre, and J. Conradi, "Properties of avalanche photodiodes," *RCA Review*, vol. 35, pp. 234–278, Jun. 1974.
[28] L. Wang, S. Jacques, and L. Zheng, "MCML, Monte Carlo modeling of light transport in multi-layered tissues," Tech. Rep., Laser Biology Research Laboratory, University of Texas, M.D. Anderson Cancer Center, Nov. 1995.
[29] B. Cochenour, L. Mullen, and J. Muth, "Effect of scattering albedo on attenuation and polarization of light underwater," *Opt. Lett.,* vol. 35, no. 12, pp. 2088–2090, 2010.
[30] H. Ding, G. Chen, A. Majumdar, B. Sadler, and Z. Xu, "Modeling of non-line-of-sight ultraviolet scattering channels for communication," *IEEE J. Sel. Areas Commun.*, vol. 27, no. 9, pp. 1535–1544, Dec. 2009.
[31] G. Zaccanti, P. Bruscaglioni, and M. Dami, "Simple inexpensive method of measuring the temporal spreading of a light pulse propagating in a turbid medium," *Appl. Opt.*, vol. 29, no. 27, pp. 3938–3944, Sept. 1990.
[32] J. G. Proakis and M. Salehi, *Digital Communications*, 5th ed. McGraw-Hill Inc., 2007.

Shijian Tang (S'11) received the B.S. degree in electronics and communication engineering from Tianjin University in 2011, and now is pursuing his M.S. degree in electronic engineering from Tsinghua University. From Sept. 2011 to Jul. 2014 (expected), he serves as the Graduate Research Assistant in Modern Communication Laboratory in Tsinghua Graduate School. From Jul. 2013 to Mar. 2014 (expected), he is an Intern Research Assistant in Potevio Institute of Technology, Co., Ltd. His research interests include channel modeling and system design of free space optical communications such as underwater wireless optical communications, visible light communications and ultraviolet NLOS communications, as well as physical layer design of LTE-based systems.

Yuhan Dong (S'07–M'10) received the B.S. and M.S. degrees in electronic engineering from Tsinghua University, Beijing, in 2002 and 2005 respectively, and the Ph.D. degree in electrical engineering from North Carolina State University, Raleigh, NC, in 2009. From 2002 to 2005, he was a Graduate Research Assistant with Complex Engineered Systems Laboratory at Tsinghua University. From 2006 to 2009, he was a Graduate Research Assistant with Wireless Systems Engineering (WiSE) Laboratory at North Carolina State University. Since January 2010, he has been with the Graduate School at Shenzhen, Tsinghua University, where he is currently an Assistant Professor and member of Modern Communication Laboratory. His research interests include the general area of wireless communications and networking, digital signal processing, antenna design, and sensor networks. He was the recipient of the 2008 IEEE GLOBECOM Best Paper Award.

Xuedan Zhang received his B.S. degree in telecommunication engineering from Beijing University of Posts and Telecommucation, Beijing, in 2002, and his Ph.D. degree in electronic engineering from Tsinghua University, Beijing, in 2008. Since January 2010, he has been with the Graduate School at Shenzhen, Tsinghua University and currently served as an Assistant Professor in Modern Communication Laboratory. His research interests include the general area of wireless communications and networking, and intelligent transportation system.